J. Membrane Biol. 74, 203–215 (1983)

The Journal of
Membrane Biology

Effect of Several Uncouplers of Cell-to-Cell Communication on Gap Junction Morphology in Mammalian Heart

J. Délèze and J.C. Hervé
Physiologie Cellulaire, Laboratoire Associé au CNRS no 290, Université de Poitiers, 86022 Poitiers, France

Summary. Electrical conduction in sheep Purkinje fibers has been blocked by three different procedures: (I) 1 mM 2-4-dinitrophenol, (II) 3.5 mM *n*-Heptan-1-ol (heptanol), and (III) treatment by a hypotonic (120 mOsmoles) Ca^{2+}-free solution for half an hour, followed by return to normal conditions. The gap junction morphology was analyzed quantitatively in freeze-fracture replicas and compared in electrically conducting and nonconducting fibers. It is found that the three uncouplers of cell-to-cell conduction induce consistent and statistically significant alterations of the gap junction structure. The investigated morphological criteria: (a) P-face junctional particle diameter, control value 8.18 ± 0.70 nm (mean $\pm$ SD), (b) P-face junctional particles center-to-center spacing, control value 10.23 ± 1.57 nm, and (c) E-face pits spacing, control value 9.45 ± 0.98 nm, are, respectively, decreased to 7.46 ± 0.62 nm, 9.25 ± 1.34 nm and 8.67 ± 1.13 nm in Purkinje fibers with complete conduction blocks. All three gap junctional dimensions are seen to decline progressively with time from the onset of an uncoupling treatment towards stable minima reached in half an hour. The observed morphological transitions appear related to the electrical uncoupling for the following reasons: partial electrical uncoupling results in values of the gap junctional dimensions that are intermediate between those measured in electrically coupled and uncoupled preparations, and the three morphological indices are seen to increase again towards control values very soon after electrical conduction has been re-established. It is concluded that the junctional channels closure on electrical uncoupling correlates with a measurable (-0.72 ± 0.01 nm, difference of the means $\pm$ SE) decrease of the junctional particle diameters.

Key Words Cell-to-cell conduction · conduction block · electrical uncoupling · gap junction · junctional channels · quantitative freeze-fracture EM · heart · *n*-Heptan-1-ol

Introduction

When the electrical constants of Purkinje fibers were measured by applying cable theory (Weidmann, 1952), the values of the length constant (1.9 mm) and of the myoplasm specific resistance (105 Ωcm) clearly indicated that the cytosols of the unit cells (Purkinje, 1845; Truex & Copenhaver, 1947; Caesar, Edwards & Ruska, 1958) are interconnected to form a conducting core functionally similar to that of a giant axon (Hodgkin & Rushton, 1946). The same conclusion has been extended to heart muscle cells by Woodbury and Crill (1961). Barr, Dewey and Berger (1965), Dreifuss, Girardier and Forssmann (1966) and Muir (1967) presented experimental results designating the nexus (Dewey & Barr, 1962, 1964) as a plausible site for cell-to-cell current flow in heart. When the nexal membranes were shown separated by a narrow gap accessible to extracellular lanthanum and spanned by hexagonal arrays of unstained subunits (Revel & Karnovsky, 1967) also detectable by negative staining (Benedetti & Emmelot, 1965, 1968), the membrane-associated particles seen in freeze-fractured gap junctions (McNutt & Weinstein, 1970) emerged as the wanted connecting elements between electrically coupled cells (the "connexons," Caspar, Goodenough, Makowski & Phillips, 1977).

Work on healing-over in the heart (Délèze, 1962, 1965, 1970) provided the first indications that the communicating heart cell junctions may be switched to a nonconducting state when the intracellular Ca^{2+} concentration is allowed to rise and this phenomenon, hereafter referred to as electrical uncoupling, now appears to be a general property of coupled cells (Loewenstein, 1966; Loewenstein, Nakas & Socolar, 1967; Oliveira-Castro & Loewenstein, 1971; Peracchia & Dulhunty, 1976; Rose & Rick, 1978; Ramón & Zampighi, 1980; Loewenstein, 1981). The related hypothesis that the junctional membrane permeability is determined by the cytoplasmic Ca^{2+} concentration ($[Ca^{2+}]_i$) (Loewenstein, 1966) has been supported most directly by experiments in which electrical coupling and $[Ca^{2+}]_i$ were simultaneously monitored at the same cell junction (Rose & Loewenstein, 1976).

In the septate junction of the crayfish axon,

the average size and distance of the junctional particles were seen to decrease after electrical uncoupling (Peracchia & Dulhunty, 1976). Gap junctions of mammalian liver and stomach cells showed analogous structural changes when submitted to uncoupling treatments (Peracchia, 1977) and this observation was extended to the isolated gap junctions of the calf eye lens transferred from a Ca^{2+}-free to a Ca^{2+}-containing medium (Peracchia, 1978; Peracchia & Peracchia, 1980*a*). Two recent studies have confirmed the decrease of junctional particle spacing on uncoupled mammalian heart cells, but have reported contradictory data on particle diameters, which were seen to increase at short times after the onset of uncoupling treatments (Dahl & Isenberg, 1980; Shibata & Page, 1981). The interest in an accurate description of the conformational changes of electrically uncoupled gap junctions pertains to recent molecular models of junctional particles viewed as cylindrical proteic oligomers containing a transcellular hydrophilic channel (McNutt & Weinstein, 1970, 1973; Caspar et al., 1977; Makowski, Caspar, Philipps & Goodenough, 1977) able to turn off. If the postulated closure mechanism operates by rotation and tilt of six rod-like subunits (Unwin & Zampighi, 1980), the junctional particles can be expected to shrink when the gap junctions are converted to a nonconducting form. This research is a further attempt to examine quantitatively the correlations between some morphological features of the gap junctions of heart Purkinje fibers and the state of cell-to-cell conduction, using three different procedures leading eventually to a complete loss of electrical coupling. A statistically significant decrease in junctional particle size and spacing is found at all times with all three uncoupling procedures. These results have been reported in a preliminary form (Hervé & Délèze, 1982; Délèze & Hervé, 1983*a*, *b*).

Materials and Methods

Preparations

Purkinje fibers were excised from the left ventricle of sheep hearts obtained at a slaughterhouse and stored at room temperature in Tyrode's solution containing (in mM): 5 glucose, 137 NaCl, 1.8 $CaCl_2$, 1 $MgCl_2$, 12 $NaHCO_3$, 0.4 NaH_2PO_4 and 5.4 KCl, instead of 2.7, to prevent spontaneous activity (Vassalle, 1965). The solutions were saturated with a 5% CO_2 in O_2 mixture giving a pH of 7.2. All experiments were performed at 35 °C.

Estimation of Electrical Coupling

The unit cells of a typical Purkinje fiber, delineated in the *camera lucida* drawing of Fig. 1*a*, are irregular in shape and size

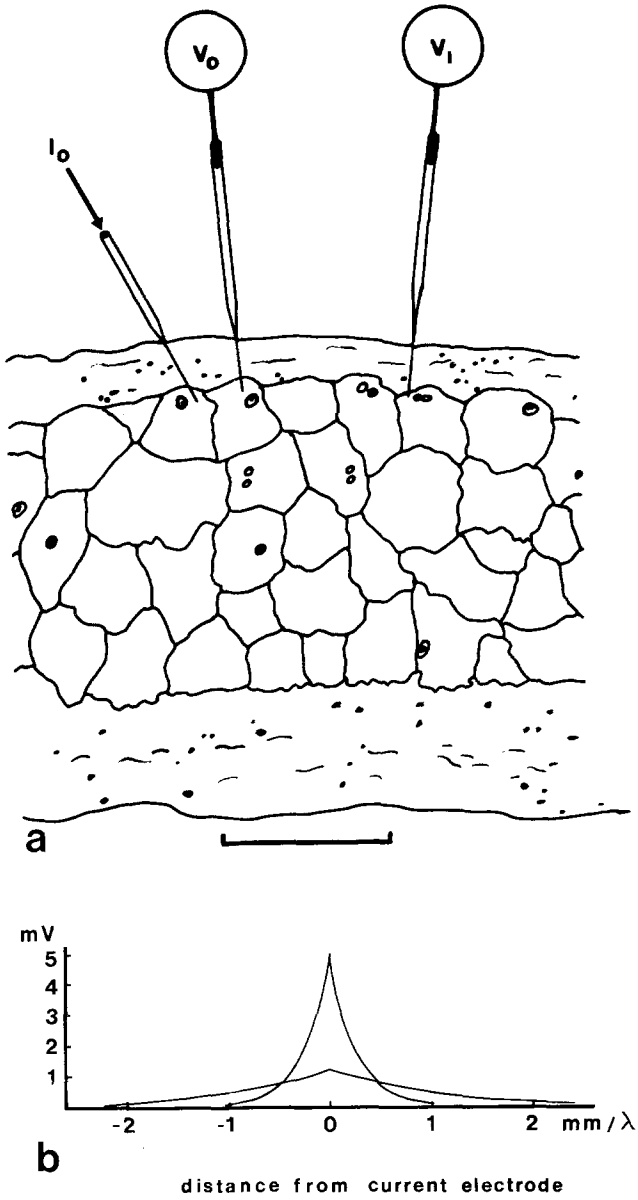

Fig. 1. (*a*) *Camera lucida* drawing of the cell boundaries in a longitudinal section of a sheep Purkinje fiber with approximate position of current-passing electrode (I_o) and recording electrodes (V_o; V_1). Scale 100 μm for Purkinje fiber. (*b*) Theoretical change in the potential distribution induced by currents of the same intensity when λ decreases from 1 (curves with the lowest maximum) to $^1/_4$ (curves with the highest maximum) in the same cable

with average dimension $h = 30$ μm measured parallel to the long axis of the functional cable. These cells are arranged in 3 to 8 rows on a cross-section and bounded by connective tissue. According to Mobley and Page (1972), gap junctions occupy 17% of the total cell membrane surface.

Applying cable equations to this multicellular structure, the progressive increase in r_i, the core resistance of one unit length of fiber, expected in the process of uncoupling can be evaluated from the shorter value of the length constant $\lambda = (r_m/r_i)^{1/2}$, where r_m is the membrane resistance of one unit length of fiber, and from the increased height of the input resistance

Table. Statistical parameters of measurement samples obtained from gap junctions of conducting and nonconducting Purkinje fibers

State of electrical coupling	Corresponding histogram	P-face particle diameters		P-face particles spacings		E-face pits spacings	
		N[a]	mean ± SD[b]	N	mean ± SD	N	mean ± SD
coupled cells	Fig. 6	8401	8.18 ± 0.70	5975	10.23 ± 1.57	7000	9.45 ± 0.98
uncoupled cells (1 mM DNP)	Fig. 8*a*	5017	7.35 ± 0.58	4082	9.32 ± 1.39	2513	8.67 ± 0.98
uncoupled cells (osmotic transition)	Fig. 8*b*	1858	7.55 ± 0.58	1289	9.08 ± 1.38	1001	8.42 ± 0.97
uncoupled cells (heptanol)	Fig. 8*c*	2074	7.53 ± 0.58	1665	9.21 ± 1.18	3197	8.76 ± 1.26
all uncoupled cells	Fig. 6	8949	7.46 ± 0.62	7036	9.25 ± 1.34	6711	8.67 ± 1.13
partially coupled cells (0.5 mM DNP)	Fig. 10	1439	7.80 ± 0.69	715	9.91 ± 1.73	727	9.07 ± 0.91
recoupled cells (after heptanol uncoupling)	Fig. 12	1250	7.73 ± 0.62	1273	9.72 ± 1.52	838	9.01 ± 1.02

[a] Number of measurements. [b] Standard deviation.

diluted with H_2O to maintain the tonicity of normal Tyrode (260 mOsmoles). After a definite morphological alteration had been established in group II (Figs. 6 & 8), a number of fibers were also fixed at intermediate stages of electrical uncoupling (Figs. 9 & 10). Finally, other preparations were fixed soon after recovery of electrical coupling (Figs. 11 & 12). The fixed specimens were immersed in a 10, 20 and 30% series of glycerol solutions in H_2O. Freeze-fracturing was carried out at −120 °C under a vacuum of 7×10^{-7} to 1×10^{-6} Torr in a Balzers BAF 300 apparatus. To minimize possible irregularities in the thickness of the shadowing material, 3 specimens from fibers in different experimental conditions were platinized simultaneously. After carbon evaporation, the replicas were coated with a drop of 1% collodion in amyl-acetate. The tissue was then digested in a commercial bleach and the replicas were washed in deionized water and collected on 400-mesh grids. The collodion film was removed by immersion in methanol.

Replicas were examined with a Hitachi HU 11 CS or a Jeol 100 C electron microscope. The magnifications used were standardized with a carbon-grating (no. 1002, E.F. Fullam). On all micrographs, the direction of platinum shadowing is from bottom to top and denomination of fracture faces follows the accepted convention (Branton et al., 1975).

Quantitative Analysis

Three morphological dimensions of the gap junctions were analyzed on fracture faces of 34 Purkinje fibers from 25 sheep hearts: *(I) P-face particle diameters* measured at the base of the particles perpendicularly to the shadowing direction. Only the particles with free edges at the base were selected for measurement. Particles whose bases were confluent or showed a common edge were rejected. Figures 5 (*b*) and (*c*) illustrate this selection procedure of the measured particles. *(II) Center-to-center distances of P-face particles* measured between particles chosen at random and all their nearest neighbors, including the tightly packed or confluent ones. *(III) Center-to-center spacings of E-face pits.*

About 400 measurements were taken for each of these three dimensions in 93% of the evaluated junctions. The remaining 7% were small surface junctions in which this number of measurements could not be reached, but the average values obtained still fell within the range for the larger junctions and have therefore been included in the pooled results (Table).

Measurements were performed on positive prints (shadows white) at a final magnification equal to 300,000× by means of a Carl Zeiss TGZ3 particle size analyzer which was set to distribute the measurements into 0.6 nm classes.

Results

Gap Junctions in Electrically Conducting Purkinje Fibers

On P-faces of freeze-fractured Purkinje fibers with normal conduction, the arrays of gap junctional membrane particles vary in size and shape from

Fig. 5 (*facing page*). (*a*) Freeze-fracture replica of a Purkinje fiber fixed in a state of normal electrical conduction. The gap junctions appear as a lattice of particles on the cytoplasmic leaflet (P-face) and complementary pits on the exoplasmic leaflet (E-face). Notice the presence of a caveola in a particle-free area inside the gap junction. Magnification 60,000×. (*b*) Part of a gap junction from another preparation with normal conduction showing a central depression, which might correspond to the opening of an axial hydrophilic channel, on most particles. Magnification 300,000×. (*c*) Enlarged drawing of six particles from the area within the frame on Fig. 5*b* to illustrate the selection and measurement procedure of P-face particle diameters. Dimensions of the particle base such as *D*, perpendicular to the shadowing direction (open arrow at right), are considered accurate measurements of the diameter if the edges of the particle shadow can be precisely delineated such as in particles *c* and *f*. Diameters of particles with confluent bases such as *d* and *e*, or with a common edge such as *a* and *b*, were not measured but their center-to-center distances, such as *S*, could be

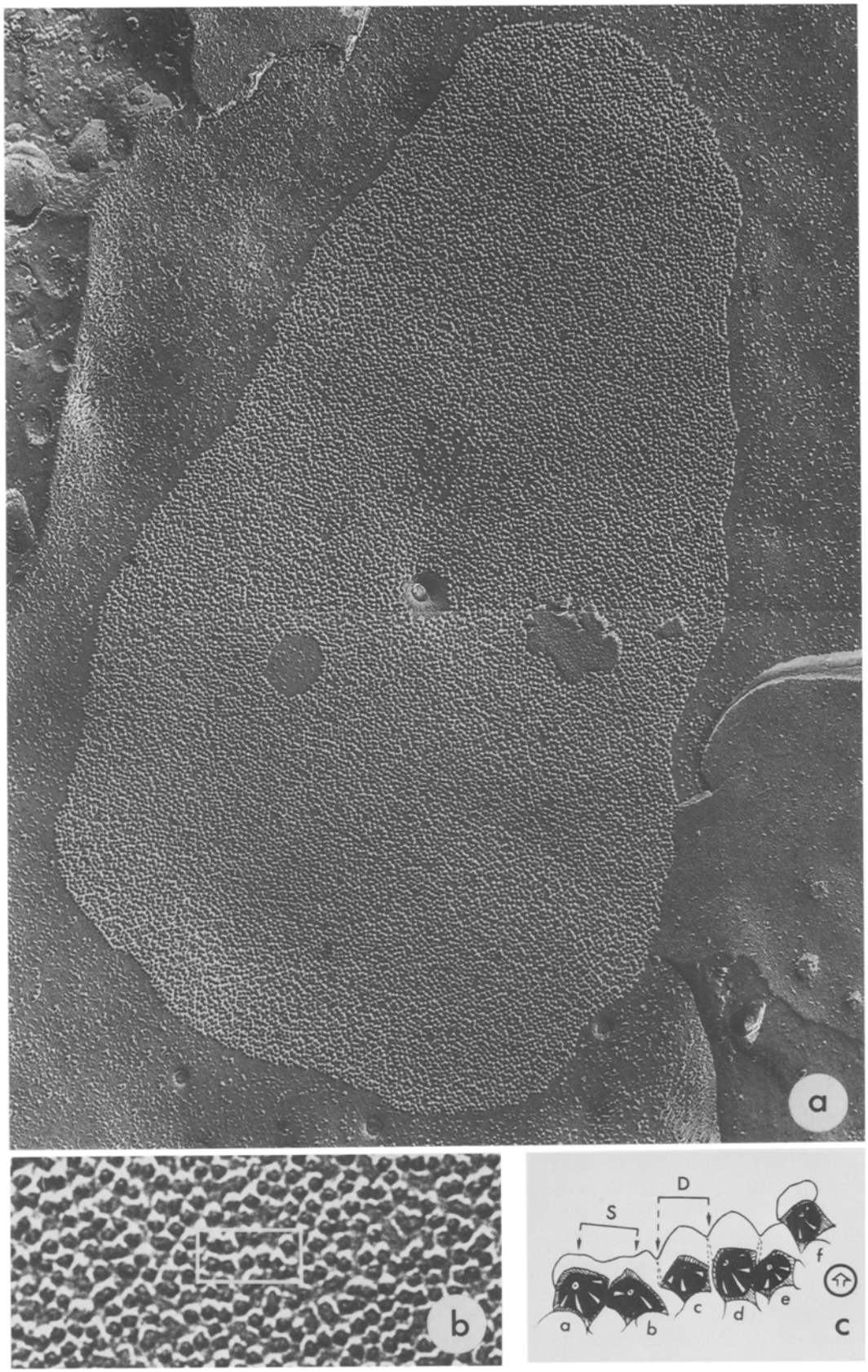
a
b
S
D
a
b
c
d
e
f
c

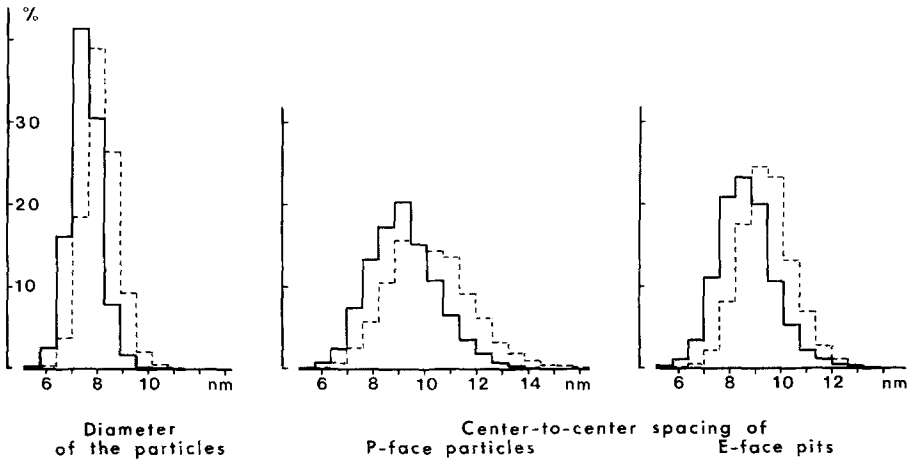

Fig. 6. Size distributions of the gap junctional dimensions: particle diameters, particles spacings and pits spacings. The dotted lines give the values obtained in control conditions and the continuous lines the values after complete electrical uncoupling. *See* Table for the statistical parameters

small clusters of a few units up to patches 5 to 10 μm^2 in area (Fig. 5*a*) made up of smaller groups more or less completely separated by particle-free aisles of smooth membrane. In some areas, small depressions, which might correspond to the openings of the hypothetic axial channels (McNutt & Weinstein, 1973), are apparent in the center of most particles (Fig. 5*b*). Our quantitative analysis of 35 gap junctions from 13 conducting Purkinje fibers is presented in the histograms of Fig. 6 (dashed lines). The distribution of P-face particle diameters is nearly symmetrical around a mean ($\pm$SD) of 8.18 ± 0.70 nm. In contrast, the center-to-center spacings of these particles (Fig. 6, center) are asymmetrically distributed with a slight positive skewness and a mean (10.23 ± 1.57 nm) which does not correspond to the modal class (9 to 9.6 nm). This type of distribution could be accounted for by two frequencies maxima at 9.2 and 11 nm, respectively, but this suggestion is not confirmed by the histogram of the E-face pits distances, which is approximately symmetrical around an average of 9.45 ± 0.98 nm (Fig. 6, right).

Gap Junctions in Electrically Uncoupled Purkinje Fibers

Even a careful inspection of the gap junctions on freeze-fracture faces from nonconducting (group II) fibers (Fig. 7) fails to detect any systematic difference with the pictures of coupled cells (Fig. 5). But the frequency distributions of the three investigated dimensions are shifted towards smaller values (Fig. 6, continuous lines, pooled data, 31 gap junctions from 14 fibers uncoupled by the three means described in Materials and Methods), when compared to the measurements obtained from coupled cells (Fig. 6, dashed lines). The respective averages of particle diameters, particle spacings and pits spacings in nonconducting fibers are reduced to 7.46 ± 0.62, 9.25 ± 1.34, and 8.67 ± 1.13 nm, which are all significantly different from the means obtained in conducting fibers ($P < 0.001$ in each uncoupled sample, where P is probability for the observed differences in averages to have arisen by chance in a normally distributed population).

It is noteworthy that all three uncoupling procedures considered separately (DNP, osmotic transition, heptanol) induce a significant ($P < 0.001$) decrease of the means which has nearly the same size inside each dimension tested (Table). This justifies the addition of the three samples performed in Fig. 6 and the Table. The shifts of the frequency distributions towards smaller classes is also very similar with the three uncoupling treatments (Fig. 8). Figures 6 and 8 also show that the shapes of the distributions are not consistently altered after uncoupling.

Change of Gap Junctional Morphology with Duration of Uncoupling Treatment

To define the evolution of the gap junction morphology while uncoupling sets in, we fixed a number of Purkinje fibers after different durations of DNP (1 mM) treatment. Figure 9 shows that after a latency of about 5 min, our three morphological indices start to decrease monotonously towards minima reached in about 30 min. The mean r_i is still at control values in 2 preparations fixed at 5 min, when morphology is not yet altered (Fig. 9). In the fiber fixed at 10 min, r_i reaches about 4.5× its initial value of 1.8 MΩ. From 15 min onward, the elevated values of r_i are difficult to measure accurately and all preparations are therefore considered completely uncoupled.

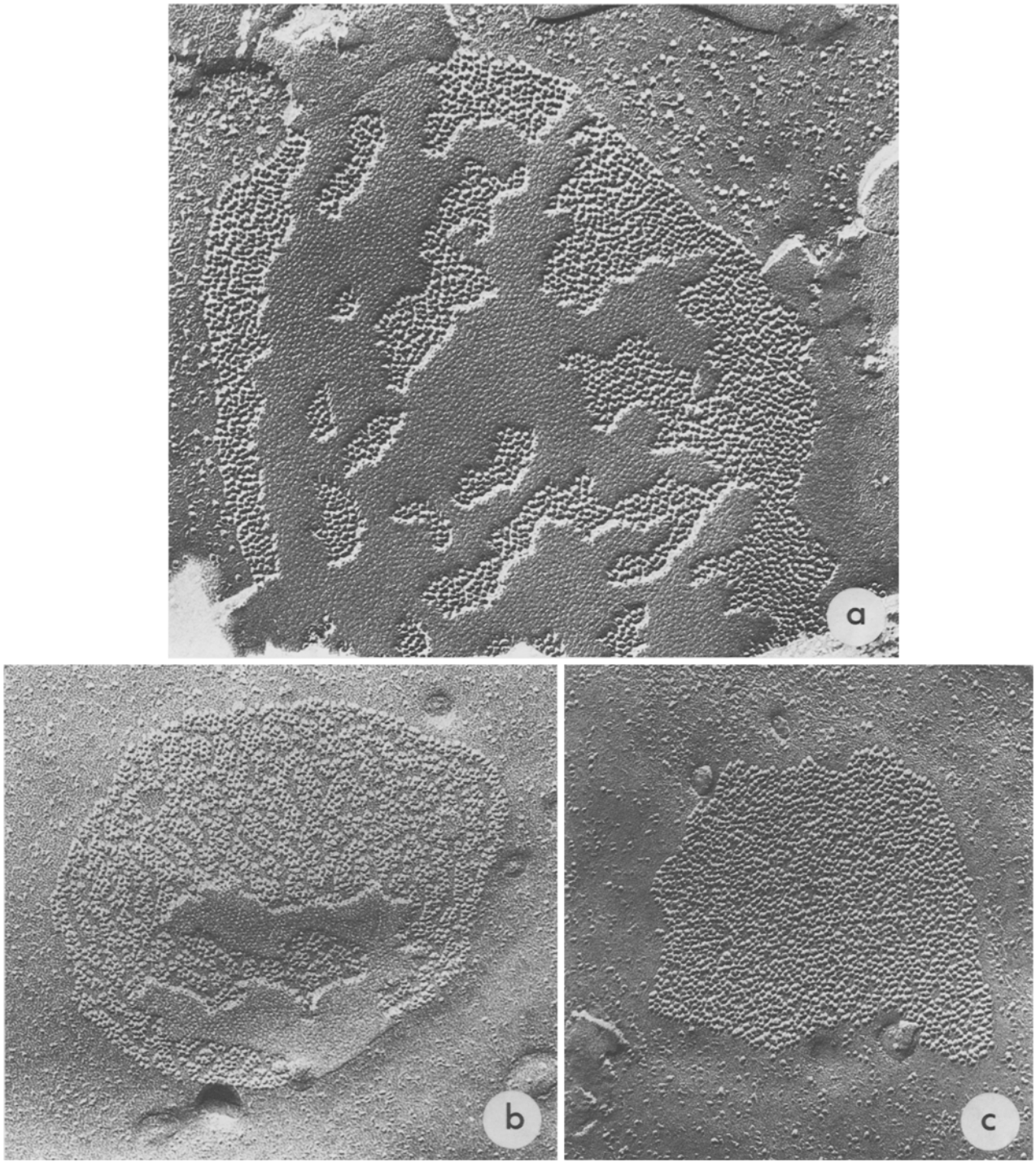

Fig. 7. Freeze-fracture replicas of gap junctions from electrically uncoupled preparations after: (*a*) 1 mM DNP, (*b*) osmotic transition, and (*c*) 3.5 mM heptanol. In some parts of (*b*), the junction appears divided into areas of tightly clustered particles alternating with particle-free aisles of smooth membrane. Magnification 110,000 ×

Gap Junctional Morphology in a Partially Coupled Purkinje Fiber

Treatment of Purkinje fibers with 0.5 mM DNP often induced a rather stable state of partial coupling similar to that observed transitorily during the action of 1 mM DNP or 3.5 mM heptanol (*see* example in Fig. 3 at 8 min), but long enough in duration to allow fixation at a well-defined value of electrical coupling. Figure 10 shows the results of one experiment in which a Purkinje fiber treated with 0.5 mM DNP was fixed at 53 min when r_i had been stable at about 18 × its initial value for the last 30 min. Comparison of Figs. 10 and 6 shows

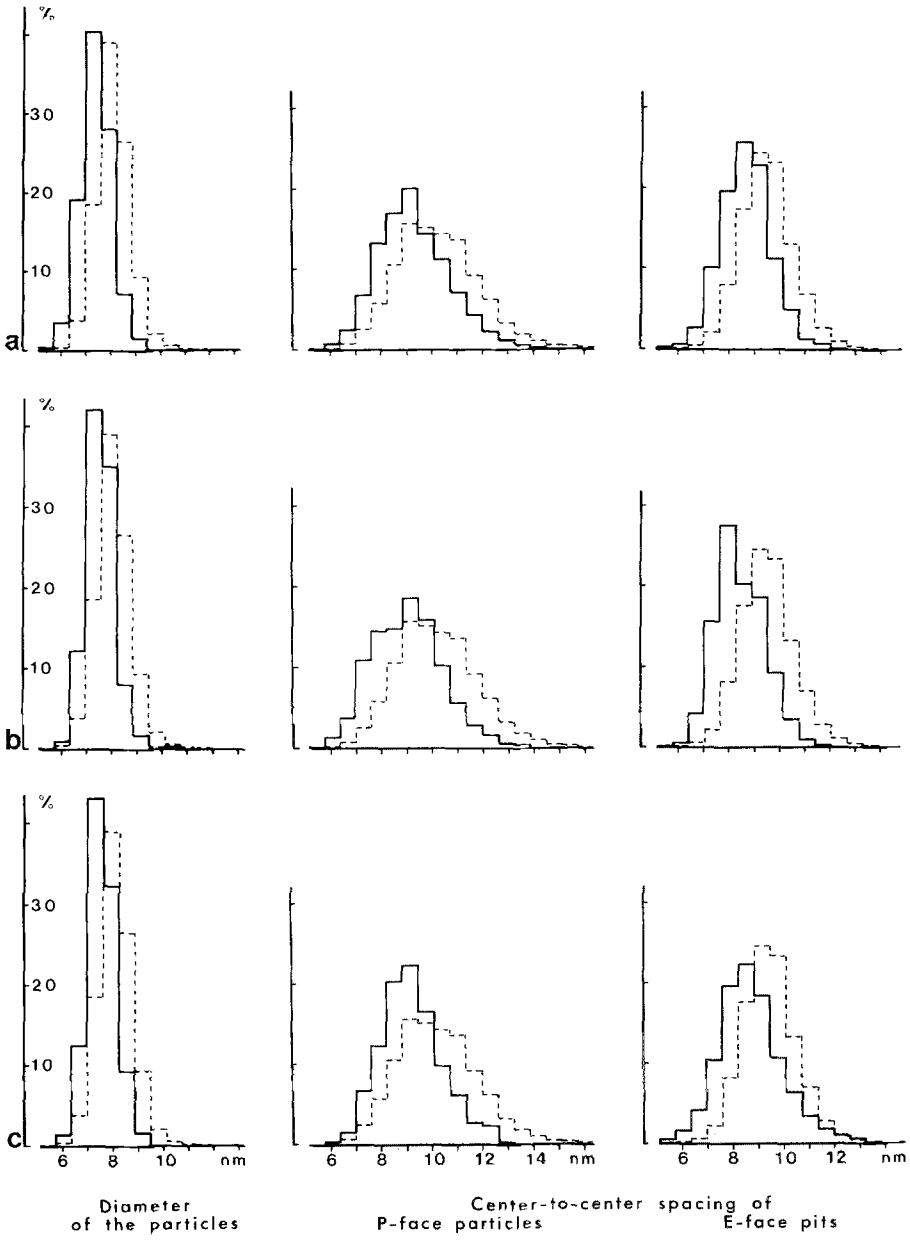

Fig. 8. Histograms showing the changes in size distributions of the gap junctional dimensions after three uncoupling procedures: (*a*) 1 mM DNP, (*b*) osmotic transition, and (*c*) 3.5 mM heptanol. *See* Table for the statistical parameters. The histograms of the control state (from Fig. 6) are repeated in dotted lines for comparison

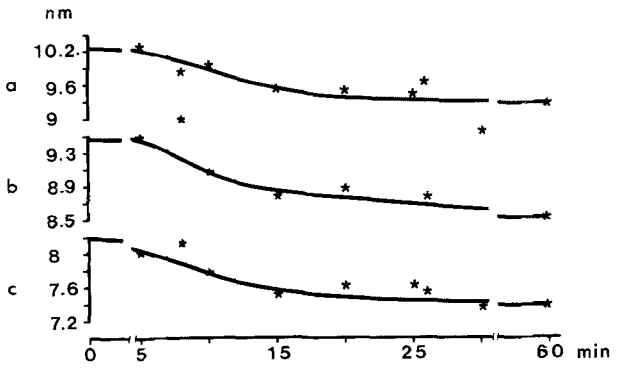

Fig. 9. (*a*) P-face particle spacings, (*b*) E-face pits spacings, and (*c*) particle diameters as functions of time after the onset of DNP-treatment (1 mM). All points give the mean measurements of several gap junctions from one fiber, except points at 5 and 20 min which were obtained from two fibers

that the shift of the gap junctional dimensions towards smaller values is less in partially coupled than in completely uncoupled preparations. This suggestion of an intermediate state of gap junction morphology is supported by the mean values of particle diameters, particles spacings and pits spacings, which are nearly midway between the averages obtained for conducting and nonconducting fibers (Table).

Gap Junctional Morphology in an Electrically Recoupled Purkinje Fiber

Returning Purkinje fibers to Tyrode's solution after complete electrical uncoupling by heptanol restores cell-to-cell communication in 10 to 15 min.

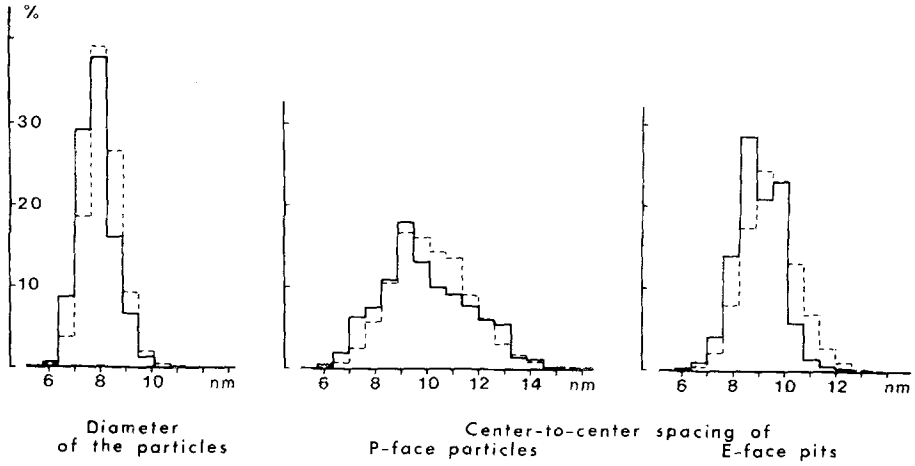

Fig. 10. Histograms of the three gap junctional dimensions from a preparation in a partially coupled state after applying 0.5 mM DNP for 53 min. *See* Table for the statistical parameters. The histograms of the control state (from Fig. 6) are repeated in dotted lines for comparison

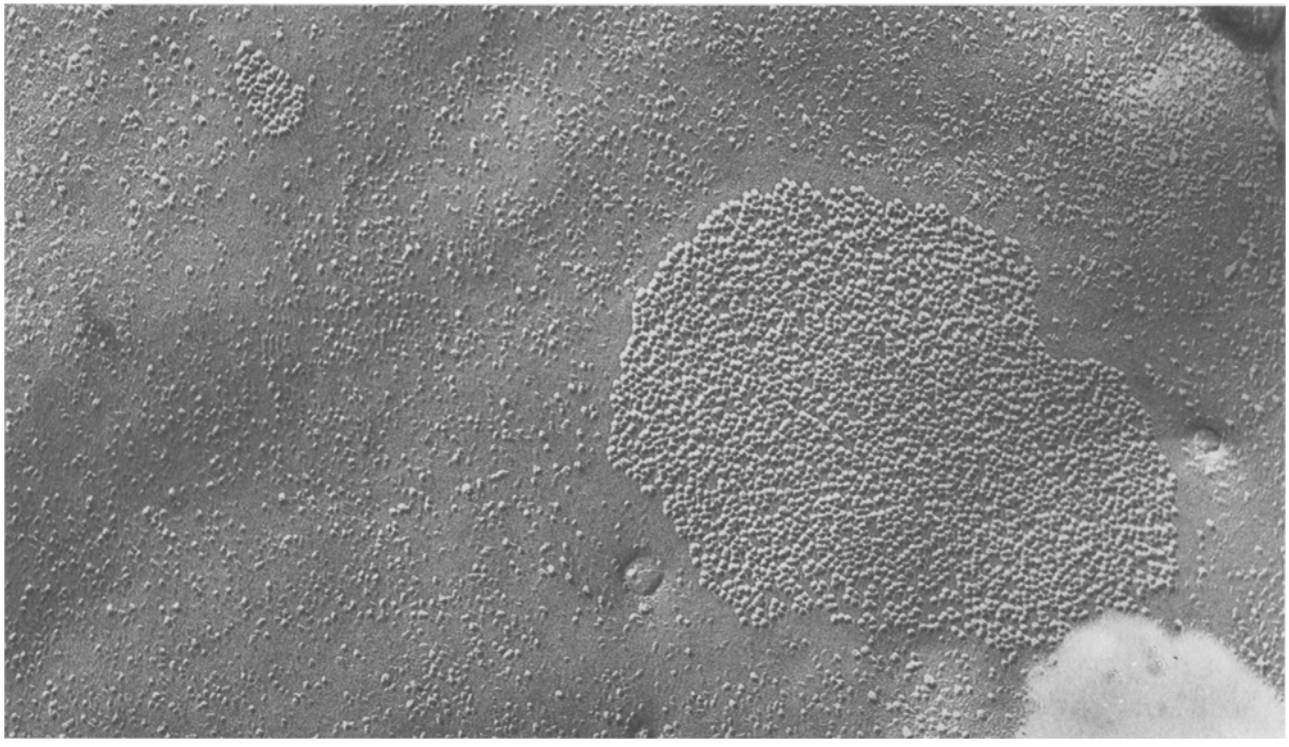

Fig. 11. Freeze-fracture replica of gap junctions from a preparation fixed 6 min after electrical coupling had recovered from a complete conduction block in 3.5 mM heptanol. Magnification 110,000 ×

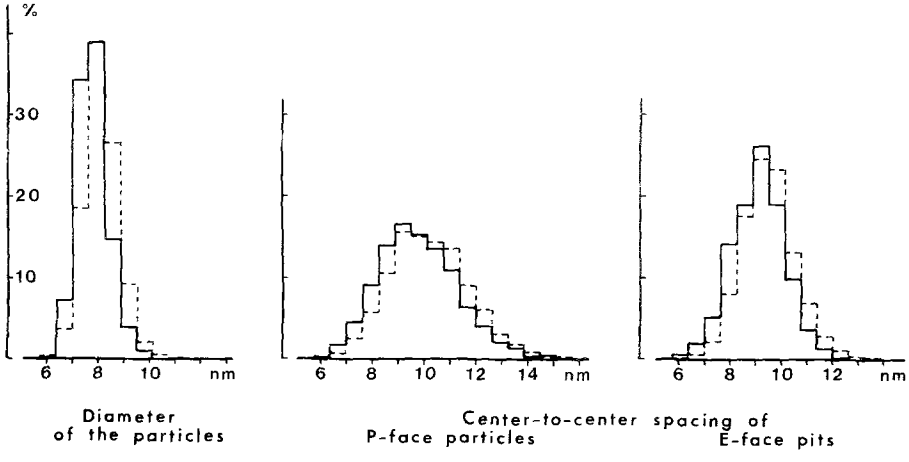

Fig. 12. Histograms of the gap junctional dimensions from a preparation fixed 6 min after electrical coupling had recovered from a complete conduction block in 3.5 mM heptanol. *See* Table for the statistical parameters. The histograms of the control state (from Fig. 6) are repeated in dotted lines for comparison

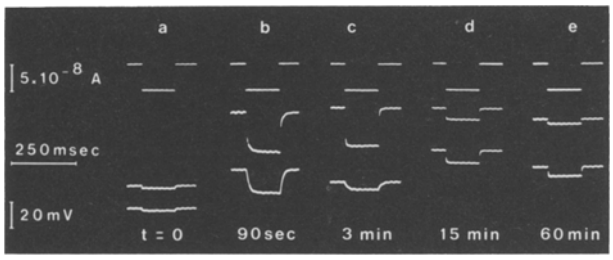

Fig. 13. Transitory increase of input resistance during fixation of a Purkinje fiber by 1.25% glutaraldehyde in Tyrode's solution. *From top to bottom:* current calibration, V_0 at 90 μm and V_1 at 150 μm from the point of current application. The initial value of r_i in Tyrode ($t=0$) is 909 KΩ. The rapid rise of input resistance observed at the onset of chemical fixation is caused by increases of r_i and r_m. It can be seen that uncoupling is never complete (*compare* Fig. 3) and that r_i decreases later on. *See* text for quantitative estimates of r_i and r_m in glutaraldehyde

Figure 11 shows an example of gap junction from a preparation fixed 6 min after complete recovery of electrical coupling. The corresponding quantitative analysis presented in Fig. 12 (continuous line) and the Table allows the conclusion that the three investigated dimensions take values which are, like those obtained in a partially coupled fiber, approximately midway between the data collected from conducting and nonconducting fibers.

Discussion

Effects of Chemical Fixation on Junctional Conductance

The electrical conductance of the crayfish electrical synapse quickly decreases at the onset of glutaraldehyde fixation and rises again later on (Politoff & Pappas, 1972). Control experiments preliminary to this research have shown an analogous effect of our fixation fluid (1.25% glutaraldehyde in Tyrode's solution) applied to normally conducting Purkinje fibers, which was not altered by omitting Ca^{2+} and replacing NaCl by K_2SO_4. In the typical experiment shown in Fig. 13, chemical fixation induces a permanent increase of the surface membrane resistance by a factor 7 to 10×. The core resistance also increases very rapidly at first, reaching a peak about 100× its control value three minutes after the onset of fixation and then gradually decreases towards a rather steady size, reached at about 15 min, of the same order as the prefixation control. But even when the internal resistance attained its peak, a definite cell-to-cell transmission was still maintained and uncoupling never reached the same degree as after DNP or heptanol treatment (*compare* Fig. 3 at 30 min and Fig. 13 at 3 min). It may therefore be presumed that communicating junctions can be fixed by chemical means in a partial, if not in a completely normal, conducting state. This assumption is strengthened by the observation of well-defined morphological differences in the gap junctions of electrically coupled and uncoupled cells that are qualitatively and quantitatively similar when using different uncoupling procedures (Table). This consistency of the observed morphological alterations is most simply accounted for by admitting a genuine structural change related to the degree of electrical uncoupling. Other possible explanations, such as differences in the efficiency of glutaraldehyde fixation, appear less likely because, to explain our morphological observations, they would have to produce very similar effects after the three quite different uncoupling treatments that have been employed.

However, the fact remains that the junctional conductance undergoes an important decrease during the first minutes of chemical fixation and that its later recovery cannot be safely interpreted. It would therefore be interesting to re-examine the structure-function correlations in gap junctions from tissues fixed by quick-freezing instead of chemicals.

Accuracy of Particle Diameters

Our selection criteria of the junctional particles for measuring the diameters (Fig. 5*c*) eliminate the particles showing confluent bases or common edges, in which the largest errors would be expected. This procedure may also reduce the effect of variations in platinum thickness dependent on particle closeness, since most measurements are taken outside the tightly packed areas. Admittedly, a large number of particles are thus not taken into account, but there is no way to measure them accurately with this technique and there is no reason to expect that they belong to a different population.

Uncoupling Mechanisms

Three different uncoupling procedures were tried with the idea that consistent effects on the gap junctional morphology would increase the probability for the change in configuration to be causally linked to the loss of junctional permeability and reduce the possible incidence of trivial factors.

As indicated in Materials and Methods, the uncoupling effect of DNP on cell-to-cell communication can be accounted for simply within the frame of the Ca^{2+} hypothesis of junctional channel regulation (Loewenstein, 1966, 1981).

The reversible uncoupling effect of heptanol,

first described in the crayfish electrical synapse (Johnston et al., 1980) and also found in the *Xenopus* embryo and vertebrate tissues (Bernardini, Peracchia & Peracchia, 1982), has not been explained. The uncoupling action of this substance on the electrical synapse is shared by other aliphatic alcohols from C_6 to C_9, but not by the local anesthetics procaine, benzocaine and propanolol (Johnston et al., 1980). Diethyl ether at very large doses (1 g/100 ml) does not interrupt cell-to-cell conduction in Purkinje fibers (J. Délèze, *unpublished observations*). Heptanol thus seems to belong to a restricted class of anesthetics with a special action on junctional membranes. It is remarkable that even at a concentration of 10 mM, this substance does not increase the septal resistance of the crayfish axon when perfused internally in a Ca^{2+}-free, citrate-containing solution (Johnston et al., 1980). This observation may indicate that the heptanol effect on the electrical synapse is mediated by a rise of $[Ca^{2+}]_i$, which should be prevented by the internal perfusion. It would therefore be of interest to monitor $[Ca^{2+}]_i$ during heptanol action.

In the course of preliminary trials to render the cell membrane permeable to extracellular Ca^{2+} ions by prolonged soaking in Ca^{2+}-free, chelator-containing solutions resembling those used for "chemical skinning" of heart muscle fibers (Winegrad, 1971), it was found that electrical uncoupling never occurred unless the solutions were made hypotonic. Uncoupling then took place either in the hypotonic Ca^{2+}-free medium, or after returning to the Tyrode's solution. Very low Ca^{2+} concentrations are known to increase the heart muscle fiber membrane permeability to Ca^{2+} ions (Thomas, 1960; Winegrad, 1971) but this effect is apparently insufficient to raise the $[Ca^{2+}]_i$ above the threshold for electrical uncoupling in Purkinje fibers. It seems possible that the added mechanical strain induced by the hypotonicity further increases the cell membrane permeability and that this effect is long enough in duration for $[Ca^{2+}]_i$ to rise above the uncoupling threshold when returning to Tyrode's solution (Ca^{2+} concentration 1.8 mM). A similar action of hypotonicity on the permeability of cell organelles membranes might be postulated to account for the electrical uncoupling that sometimes occurred in the hypotonic solution itself. But these suggestions will remain speculative as long as $[Ca^{2+}]_i$ has not been monitored.

Junctional Particle Diameter

A relatively small (-0.63 to -0.83 nm) but statistically significant ($P<0.001$) decrease of junctional particle diameter is consistently obtained with all three uncoupling procedures. The size of this contraction is comparable to the difference in the dimensions of the central channel (about 10 Å) close to its cytoplasmic end as measured by Unwin and Zampighi (1980) on the two configurations, presumably corresponding to the opened and closed states, of the connexons in gap junctions isolated from rat liver, but it appears to be larger than expected from their model of rotating and tilting subunits.

Even in gap junctions from a partially coupled Purkinje fiber, the histogram of particle diameters (Fig. 10) remains nearly symmetrical around the mean. The presence of two maxima of size frequencies would be expected in partially coupled, and perhaps even in normally coupled fibers, if uncoupling were promoted by a simple all-or-none transition of particle size from an "opened" state with a well-defined larger diameter, to a "closed" state with a constant smaller size. The data in Fig. 10 are certainly compatible with a continuous-transition model, although they cannot be decisive on this point, as an existing all-or-none transition with two frequency peaks might be blurred by an insufficient resolution of our morphological analysis. However, other results clearly indicate that channel closure is a progressive phenomenon: on elevation of $[Ca^{2+}]_i$, the cell-to-cell transit of larger molecules can be slowed and even blocked while smaller molecules are still passing (Rose, Simpson & Loewenstein, 1977), and the conductance of unit cell-to-cell channels is seen to decrease either in quantal or in partial steps (Loewenstein, Kanno & Socolar, 1978).

The incomplete reversibility of particle diameters in a Purkinje fiber fixed 6 min after recovery of electrical conduction (Fig. 12 and Table) does not necessarily indicate the presence of a genuine time lag between the restorations of morphology and function, because it can be shown that r_i is not a very sensitive index of the junctional conductance when the latter approaches its high normal value (*cf.* Eq. (13) in Socolar & Loewenstein, 1979; *cf. also* Socolar, 1977).

Dahl and Isenberg (1980) report an increase of the gap junctional particle diameter in Purkinje fibers uncoupled by 15-min DNP treatment and a decrease when treatment is prolonged to 1 hr. A similar increase in diameter, which was stable in time, has been measured in Purkinje fiber gap junctions situated close to a cut in a high (1.8×10^{-3} M) Ca^{2+} concentration (Shibata & Page, 1981). In our experiments, an increase in particle size has never been observed even at short durations of DNP treatment (Fig. 9). That this dis-

crepancy could come from a bias depending on differences in experimental designs is by no means obvious. The only worth-mentioning difference in preparative techniques is our avoidance of Na-cacodylate, which in preliminary experiments had been seen to rapidly depolarize Purkinje fibers when added to the Tyrode's solution.

Our data on the change in particles spacing when heart cells uncouple are consistent with other recent reports (Baldwin, 1979; Dahl & Isenberg, 1980; Shibata & Page, 1981). The changes in the three investigated gap junctional dimensions, including P-face particle diameter and pits spacing, are in general agreement with the structural transitions described after junctional uncoupling of the crayfish electrical synapse (Peracchia & Dulhunty, 1976) and of the rat stomach and liver cells (Peracchia, 1977). Analogous structural transitions have been found in gap junctions isolated from calf lens fibers and submitted to increased Ca^{2+} (Peracchia, 1978), Mg^{2+} (Peracchia & Peracchia, 1980*a*) or H^+ (Peracchia & Peracchia, 1980*b*) ion concentrations. When given access to the myoplasm, Ca^{2+} ions are capable of binding to the heart intercalated discs (Nishiye, Mashima & Ishida, 1978) and more precisely to the nexus (Nishiye, Mashima & Ishida, 1980).

Taken together, these results indicate that the binding of Ca^{2+} ions to the gap junctions triggers a conformational transition in the connexon, which can be detected as a decrease in diameter. According to Peracchia (1980), the concomitant closer aggregation of the junctional particles might be explained by a decrease of electrostatic repulsion between neighboring particles after neutralization of fixed negative charges by Ca^{2+} ions.

We wish to thank Mme Brigitte Vincent for her skillful drawing of Fig. 5*c*.

References

Baldwin, K.M. 1979. Cardiac gap junction configuration after an uncoupling treatment as a function of time. *J. Cell Biol.* **82**:66–75

Barr, L., Dewey, M.M., Berger, W. 1965. Propagation of action potentials and the structure of the nexus in cardiac muscle. *J. Gen. Physiol.* **48**:797–823

Benedetti, E.L., Emmelot, P. 1965. Electron microscopic observations on negatively stained plasma membranes isolated from rat liver. *J. Cell Biol.* **26**:299–304

Benedetti, E.L., Emmelot, P. 1968. Hexagonal array of subunits in tight junctions separated from isolated rat liver plasma membranes. *J. Cell Biol.* **38**:15–28

Bernardini, G., Peracchia, C., Peracchia, L.L. 1982. Reversible gap junction, crystallization and electrical uncoupling by heptanol. *Biophys. J.* **37**:285a

Branton, D., Bullivant, S., Gilula, N.B., Karnovsky, M.J., Moor, H., Muehlethaler, K., Northcote, D.H., Packer, L., Satir, B., Speth, V., Staehelin, L.A., Steere, R.L., Weinstein, R.S. 1975. Freeze-etching nomenclature. *Science* **190**:54–56

Caesar, R., Edwards, G.A., Ruska, H. 1958. Electron microscopy of the impulse conducting system of the sheep heart. *Z. Zellforsch. Mikrosk. Anat.* **48**:698–719

Caspar, D.L.D., Goodenough, D.A., Makowski, L., Phillips, W.C. 1977. Gap junction structures. I. Correlated electron microscope and X-ray diffraction. *J. Cell Biol.* **74**:605–628

Dahl, G., Isenberg, G. 1980. Decoupling of heart muscle cells: Correlation with increased cytoplasmic calcium activity and with changes of nexus ultrastructure. *J. Membrane Biol.* **53**:63–75

Délèze, J. 1962. Effet des ions calcium sur le rétablissement du potentiel de repos après lésion des fibres cardiaques. *Helv. Physiol. Pharmacol. Acta* **20**:C47

Délèze, J. 1965. Calcium ions and the healing-over of heart fibres. *In:* Electrophysiology of the Heart. B. Taccardi and G. Marchetti, editors. pp. 147–148. Pergamon, Oxford

Délèze, J. 1970. The recovery of resting potential and input resistance in sheep heart injured by knife or laser. *J. Physiol. (London)* **208**:547–562

Délèze, J., Hervé, J.C. 1983*a*. Correlation of cell-to-cell electrical uncoupling in sheep Purkinje fibres with changes in gap junction morphology. *J. Physiol. (London)* **334**:58P

Délèze, J., Hervé, J.C. 1983*b*. Changements de conformation des jonctions communicantes des fibres de Purkinje de mouton lors du découplage électrique. *J. Physiol. (Paris)* (*Abstract, In press*)

De Mello, W.C. 1979. Effect of 2-4-dinitrophenol on intracellular communication in mammalian cardiac fibres. *Pfluegers Arch.* **380**:267–276

Dewey, M.M., Barr, L. 1962. Intercellular connection between smooth muscle cells: The nexus. *Science* **137**:670–672

Dewey, M.M., Barr, L. 1964. A study of the structure and distribution of the nexus. *J. Cell Biol.* **23**:553–585

Dreifuss, J.J., Girardier, L., Forssmann, W.G. 1966. Etude de la propagation de l'excitation dans le ventricule de rat au moyen de solutions hypertoniques. *Pfluegers Arch.* **292**:13–33

Hervé, J.C., Délèze, J. 1982. Quantitative ultrastructural analysis in nexuses of cardiac Purkinje fibers. *Biol. Cell* **44**:16a

Hodgkin, A.L., Rushton, W.A.H. 1946. The electrical constants of crustacean nerve fibre. *Proc. R. Soc. London B.* **133**:444–479

Johnston, M.F., Simon, S.A., Ramón, F. 1980. Interaction of anaesthetics with electrical synapses. *Nature (London)* **286**:498–500

Loewenstein, W.R. 1966. Permeability of membrane junctions. *Ann. N.Y. Acad. Sci.* **137**:441–472

Loewenstein, W.R. 1981. Junctional intercellular communication: The cell-to-cell membrane channel. Physiol. Rev. **61**:829–913

Loewenstein, W.R., Kanno, Y., Socolar, S.J. 1978. Quantum jumps of conductance during formation of membrane channels at cell-cell junction. *Nature (London)* **274**:133–136

Loewenstein, W.R., Nakas, M., Socolar, S.J. 1967. Junctional membrane uncoupling. Permeability transformations at a cell membrane junction. *J. Gen. Physiol.* **50**:1865–1891

Makowski, L., Caspar, D.L.D., Phillips, W.C., Goodenough, D.A. 1977. Gap junction structures. II. Analysis of the X-ray diffraction data. *J. Cell Biol.* **74**:629–645

McNutt, N.S., Weinstein, R.S. 1970. The ultrastructure of the nexus. A correlated thin-section and freeze-cleave study. *J. Cell Biol.* **47**:666–688

McNutt, N.S., Weinstein, R.S. 1973. Membrane ultrastructure

at mammalian intercellular junctions. *Prog. Biophys. Mol. Biol.* **26**:45–101

Mobley, B.A., Page, E. 1972. The surface area of sheep cardiac Purkinje fibres. *J. Physiol. (London)* **220**:547–563

Muir, A.R. 1967. The effects of divalent cations on the ultrastructure of the perfused rat heart. *J. Anat.* **101**:239–261

Nishiye, H., Mashima, H., Ishida, A. 1978. Binding of ^{45}Ca to intercalated discs of cardiac muscles studied by electron microscope autoradiography. *Jpn. J. Physiol.* **28**:807–817

Nishiye, H., Mashima, H., Ishida, A. 1980. Ca binding of isolated cardiac nexus membranes related to intercellular uncoupling. *Jpn. J. Physiol.* **30**:131–136

Oliveira-Castro, G.M., Loewenstein, W.R. 1971. Junctional membrane permeability: Effects of divalent cations. *J. Membrane Biol.* **5**:51–77

Peracchia, C. 1977. Gap junctions: Structural changes after uncoupling procedures. *J. Cell Biol.* **72**:628–641

Peracchia, C. 1978. Calcium effects on gap junction structure and cell coupling. *Nature (London)* **271**:669–671

Peracchia, C. 1980. Structural changes of gap junction permeation. *Int. Rev. Cytol.* **66**:81–146

Peracchia, C., Dulhunty, A.F. 1976. Low resistance junctions in crayfish. Structural changes with functional uncoupling. *J. Cell Biol.* **70**:419–439

Peracchia, C., Peracchia, L.L. 1980*a*. Gap junction dynamics: Reversible effects of divalent cations. *J. Cell Biol.* **87**:708–718

Peracchia, C., Peracchia, L.L. 1980*b*. Gap junction dynamics: Reversible effects of hydrogen ions. *J. Cell Biol.* **87**:719–727

Politoff, A.L., Pappas, G.D. 1972. Mechanisms of increase in coupling resistance at electrotonic synapses of the crayfish septate axon. *Anat. Rec.* **172**:384–385

Politoff, A.L., Socolar, S.J., Loewenstein, W.R. 1969. Permeability of a cell membrane junction. Dependence on energy metabolism. *J. Gen. Physiol.* **53**:498–515

Purkinje, J.E. 1845. Mikroskopisch-neurologische Beobachtungen. *Arch. Anat. Physiol. Leipzig.* pp. 281–295

Ramón, F., Zampighi, G. 1980. On the electrotonic coupling mechanism of crayfish segmented axons: Temperature dependence of junctional conductance. *J. Membrane Biol.* **54**:165–171

Revel, J.P., Karnovsky, M.J. 1967. Hexagonal array of subunits in intercellular junctions of the mouse heart and liver. *J. Cell Biol.* **33**:C7–C12

Rose, B., Loewenstein, W.R. 1976. Permeability of a cell junction and the local cytoplasmic free ionized calcium concentration: A study with aequorin. *J. Membrane Biol.* **28**:87–119

Rose, B., Rick, R. 1978. Intracellular pH, intracellular free Ca, and junctional cell-cell coupling. *J. Membrane Biol.* **44**:377–415

Rose, B., Simpson, I., Loewenstein, W.R. 1977. Calcium ion produces graded changes in permeability of membrane channels in cell junction. *Nature (London)* **267**:625–627

Shibata, Y., Page, E. 1981. Gap junctional structure in intact and cut sheep cardiac Purkinje fibers: A freeze-fracture study of Ca^{2+}-induced resealing. *J. Ultrastruct. Res.* **75**:195–204

Socolar, S.J. 1977. *Appendix:* The coupling coefficient as an index of junctional conductance. *J. Membrane Biol.* **34**:29–37

Socolar, S.J., Loewenstein, W.R. 1979. Methods for studying transmission through permeable cell-to-cell junctions. *In:* Methods in Membrane Biology. E. Korn, editor. Vol. 10, pp. 123–179. Plenum, New York

Thomas, L.J. 1960. Increase of labeled calcium uptake in heart muscle during potassium lack contracture. *J. Gen. Physiol.* **43**:1193–1206

Truex, R.C., Copenhaver, W.M. 1947. Histology of the moderator band in man and other mammals with special reference to the conduction system. *Am. J. Anat.* **80**:173–202

Unwin, P.N.T., Zampighi, G. 1980. Structure of the junction between communicating cells. *Nature (London)* **283**:545–549

Vassalle, M. 1965. Cardiac pacemaker potentials at different extra- and intra-cellular K concentrations. *Am. J. Physiol.* **208**:770–775

Weidmann, S. 1952. The electrical constants of Purkinje fibres. *J. Physiol. (London)* **118**:348–360

Winegrad, S. 1971. Studies of cardiac muscle with a high permeability to calcium produced by treatment with ethylenediaminetetraacetic acid. *J. Gen. Physiol.* **58**:71–93

Woodbury, J.W., Crill, W.E. 1961. On the problem of impulse conduction in the atrium. *In:* Nervous Inhibition. E. Florey, editor. pp. 124–135. Pergamon, New York

Received 30 August 1982; revised 24 January 1983